Optimal Control of Automatic Voltage Regulator System with Coronavirus Herd Immunity Optimizer Algorithm-Based PID plus Second Order Derivative Controller

*[1]Selçuk EMİROĞLU, [2]Talha Enes GÜMÜŞ

[1]Department of Electrical and Electronics Engineering, Sakarya University, Sakarya, Turkey, selcukemiroglu@sakarya.edu.tr iD

[2]Department of Electrical and Electronics Engineering, Sakarya University, Sakarya, Turkey, tgumus@sakarya.edu.tr iD

Abstract

Optimal control of the Automatic Voltage Regulator (AVR) system can improve the system behavior with the optimal parameters obtained based on optimization. The optimal design of proposed Proportional Integral Derivative (PID) and Proportional Integral Derivative plus Second Order Derivative (PIDD^2) controllers are modeled as an optimization problem including objective function and constraints. The optimization problem is solved by using the Coronavirus Herd Immunity Optimizer (CHIO) algorithm to find the best controller parameters. The optimal design of PID and PIDD^2 controllers for the AVR system is presented considering different objective functions. CHIO is inspired by herd immunity against COVID-19 disease by social distancing. The performances of CHIO-based controllers in the AVR system are compared with those of some modern well-known algorithms such as Atom Search Optimization (ASO), Opposition-Based Atom Search Optimization (OBASO), Particle Swarm Optimization (PSO), Improved Whale Optimization (IWO), Artificial Bee Colony (ABC), Kidney-inspired algorithm (KA), Differential Evolution (DE), Ziegler- Nichols (ZN), Local Unimodal Sampling (LUS), Biogeography-Based Optimization (BBO) and Pattern Search (PS) algorithms. Also, the obtained results demonstrate that the CHIO algorithm yields the least objective value in comparison with the other algorithms, and the superiority of the proposed approach is demonstrated.

Keywords: AVR; CHIO; Optimization; PIDD plus Second Order Derivative Controller

1. INTRODUCTION

Several voltage controllers automatically maintain the reactive power and voltage profile during power system operation and control, one of which is the automatic voltage regulator (AVR) [1].

A terminal voltage of a synchronous generator can be automatically controlled, adjusted, or maintained with the help of an AVR. The primary function of the AVR is to keep the voltage at generator terminals within a certain level or limits [2]. Therefore, the stability of the AVR system has a significant impact on the reliability of the power system [1]. So, the AVR system faces some issues with an insufficient oscillating transient response, maximum overshoot, more settling time, and steady-state errors.

The AVR system can maintain the terminal voltage at the desired level under closed-loop control using a Proportional Integral Derivate (PID) controller. Due to ease of implementation, simple structure, and robust performance, PID controllers are widely employed in process control [3]. Three parameters of PID controllers are generally adjusted

with the conventional methods such as Ziegler/Nichols method, pole placement, etc. [4]. However, many intelligent algorithms are applied to adjust and obtain the parameters of the controller, such as Artificial bee colony (ABC) [3], Pattern Search (PS) [3], Particle Swarm Optimization (PSO) [5], Chaotic Ant Swarm (CAS) [5], Improved Whale Optimization (IWO) [6], Kidney-inspired algorithm (KA) [7], atom search optimization (ASO) [8], opposition-based atom search optimization (OBASO) [8], hybrid simulated annealing – Manta ray foraging optimization (SA-MRFO) [9], Ziegler- Nichols (ZN) [10], grasshopper optimization algorithm (GOA) [10], local unimodal sampling (LUS) [11], biogeography-based optimization (BBO) [12], Nonlinear Sine Cosine (NSCA) algorithms, etc. due to some disadvantages of the conventional methods. Also, tuning of fractional-order PID (FOPID) controllers has also recently gained importance. FOPID differs from traditional PID controllers in that it has fractional values as the order of the derivative and integral terms [13], [14]. The PID controller has seven independent parameters are optimally tuned based on sine-cosine algorithm (SCA) by doing time-domain, frequency and robustness analysis [13]. Also, a robust FOPID controller is designed by using Cuckoo

---

* Corresponding Author

Search (CS) algorithm [14]. There are also studies using fuzzy rules for traditional PID structures called Fuzzy Logic PID (FLPID). [15]. NSCA based sigmoid PID are proposed for AVR system considering objective function with steady state error and overshoot [16]. However, a Feedback Error Learning (FEL) controller, consisting of a classical controller (PD controller) and an intelligent controller (MLP neural network controller), has been proposed for the control of the AVR system for the control of AVR system with an uncertain plant model [17]. Moreover, different type of control method, such as Sliding Mode Control (SMC) is applied for AVR system [18].

In addition, several research has recently looked into a variation of the PID regulator known as the PID plus second-order derivative term generally called $PIDD^2$ [5], [6], [8]. This controller has one more parameter than a traditional PID, which is a second-order derivative gain (K_{dd}). In this paper, the optimal design of the PID and $PIDD^2$ controllers are presented by using a recently proposed optimization algorithm in the literature namely CHIO [19]. CHIO is a population-based metaheuristic algorithm inspired by herd immunity against COVID-19 [19]. CHIO algorithm has been applied for capacited vehicle routing problem [20]. The feature selection problem in the medical diagnosis domain has been also solved with the implementation of CHIO [21]. Moreover, CHIO algorithm has been successfully used in many areas such as high renewable penetration microgrid [22] and economic dispatch problems [23] etc.

The objective of the work is the design and implementation of an efficient CHIO-based PID and $PIDD^2$ controllers for the AVR system. In the study, the design of controllers formulated as an optimization problem is achieved by using CHIO algorithm to obtain the optimal controller parameters. The choice of an appropriate objective function is critical for the controller design to get a better and desired response. So, six different objective functions widely employed in the literature are used and compared in terms of the system performance with each other considering settling time, rise time, maximum overshoot, and peak time.

2. MATERIALS AND METHODS

The optimal parameters of the AVR system are obtained by using CHIO.

2.1. Coronavirus Herd Immunity Optimizer (CHIO) Algorithm

CHIO, an efficient search algorithm for global optimization problems, is a population-based metaheuristic algorithm inspired by herd immunity against COVID-19 disease by social distancing [19].

The spread of viruses among humans is very rapid. The method of fighting viruses is to create immunity against the virus. The vaccine is used to create immunity, but a certain time is needed for vaccine production. During this period, there are two ways to fight viruses.
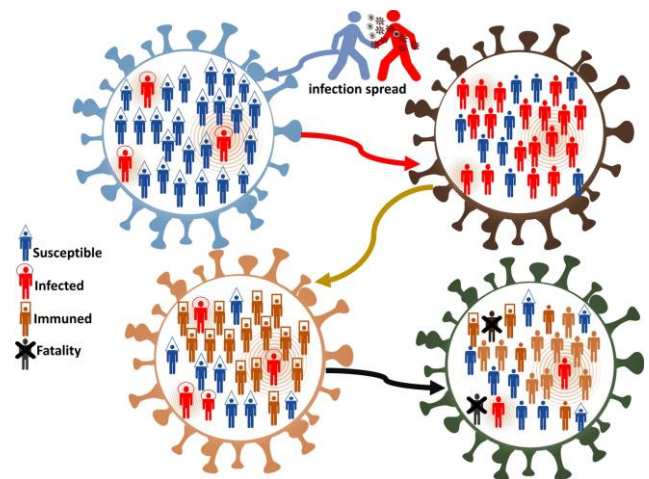
• Infected people are isolated from society.

Figure 1. Herd immunity scenario [19]

• When the majority of the population is infected, herd immunity develops against the disease, and other individuals are indirectly protected from the disease. (If a large part of the population is infected, a collective immunity is formed against the disease, and other individuals are indirectly protected from the disease as shown in Fig. 1.)

The development of herd immunity has been carried out with the COVID-19 optimization algorithm. The algorithm consists of a total of 6 steps [19]. Also, the flowchart of the algorithm is depicted in Fig. 2.

Step 1: In the first step, the objective function is created and the optimization problem is defined. CHIO includes four algorithm variables and two control parameters. The number of infected individuals (initially one), the maximum number of iterations, the population size, and the size of the problem are the parameters of the algorithm. The control variables are the rate of spread of the virus and the maximum age of the infected [19].

Step 2: Creating herd immunity population; the number and size of the population and herd immunity control variables are determined.

Step 3: Disease spread; some of the infected people here die according to the coronavirus mortality rate. These individuals cannot infect new individuals. Individuals who recover after becoming coronavirus cause the virus to spread in two ways. The first will infect according to the rate of virus spread. The latter will infect the virus according to its super spread rate [19].

Step 4: Population update: 3 populations are updated for each generation.

- Dead population: if the infected individual dies, it is added to this population and is not used again.

- Healing population: In each iteration, the infected individuals are sent to the recovered population.

- Newly infected population: In each iteration, all infected individuals are added to this population.
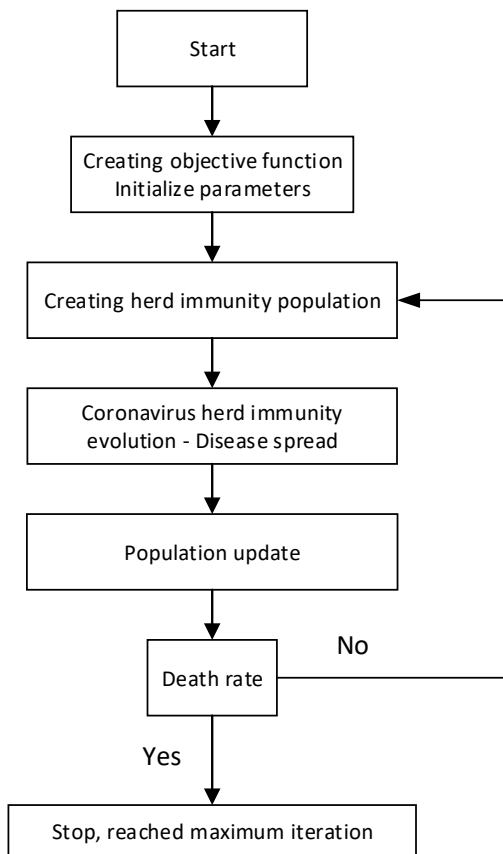
Figure 2. Flowchart of CHIO

Step 5: Mortality: If the immune rate of the infected case is not recovered for the number of iterations determined by the Maximum age parameter, this case is considered dead. This increases the existing population diversity, allowing the local outcome to move away from local minimums [19].

Step 6: Stopping criterion: The most important feature of the COVID-19 optimization algorithm is that it terminates without the need to check any parameters. This is because the recovering and dead population is constantly increasing, and newly infected individuals cannot transmit the disease to other individuals. The algorithm terminates when it reaches the maximum number of refreshes [19].

2.2. Automatic Voltage Regulator System

In power systems, the system voltage needs to be kept within the defined limit and constant. Otherwise, the system suffers stability problems, and the loads are fed by lower voltages. So, voltage drops should be prevented in power systems. AVR is designed to control and keep the terminal voltage of the generator constant. AVR controls the terminal voltage of the generator with the field current. It maintains the output voltage and keeps the voltage at the desired value. The AVR system brings the terminal voltage to the desired value under closed-loop control. AVR system contains some parts, these are an amplifier, exciter, generator, and sensor [4], [6].

a) Amplifier

The amplifier's transfer function has a gain and a time constant.

$$TF_A = \frac{K_a}{1+sT_a} \tag{1}$$

Where T_a and K_a are the time constant for the amplifier and gain, respectively. Time constant T_a is between 0.02 s and 0.1 s. The values of K_a are generally between 10 and 40 [4], [6].

b) Exciter

The transfer function for the Exciter is given as the below function. It has a time constant T_e and gain K_e. K_e and T_e values are generally between 1 and 10, and between 0.4 s and 1 s, respectively [4], [6].

$$TF_E = \frac{K_e}{1+sT_e} \tag{2}$$

c) Generator

The generator's transfer function is given below. The load affects the generator's gain and time constant. According to the load, the time constant T_g and the gain K_g are changing from 1 s to 2 s and from 0.7 to 1, respectively [4], [6].

$$TF_G = \frac{K_g}{1+sT_g} \tag{3}$$

d) Sensor

The sensor transfer function is also given as in Eq 4. T_s is between 0.001 s and 0.06 s and K_s is about 1 [4], [6].

$$TF_S = \frac{K_S}{1+sT_S} \tag{4}$$

Table 1. The parameters of the AVR system [24]

	Parameter Limits for K and T	Used Parameter Values
Amplifier	$10 \leq K_a \leq 40$ $0.02 \leq T_a \leq 0.1$	$K_a=10, T_a=0.1$ s
Exciter	$1 \leq K_e \leq 10$ $0.4 \leq T_e \leq 1$	$K_e=1, T_e=0.4$ s
Generator	$0.7 \leq K_g \leq 1$ $1 \leq T_g \leq 2$	$K_g=1, T_g=1$ s
Sensor	$1 \leq K_s \leq 2$ $0.001 \leq T_s \leq 0.06$	$K_s=1, T_s=0.01$ s

The parameters and parameter limits of the AVR system are taken as in [24] and given in Table 1.

When there is no controller, the transfer function of the AVR system as shown in Fig. 3 is expressed as follows.

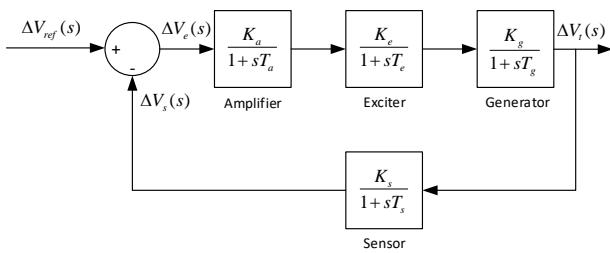$$\frac{\Delta V_t(s)}{\Delta V_{ref}(s)} = \frac{0.1s+10}{0.0004s^4 + 0.0454s^3 + 0.555s^2 + 1.51s + 11} \tag{5}$$

Selçuk Emiroğlu, Talha Enes Gümüş

Optimal Control of Automatic Voltage Regulator System with Coronavirus Herd Immunity Optimizer Algorithm-Based PID plus Second Order Derivati...

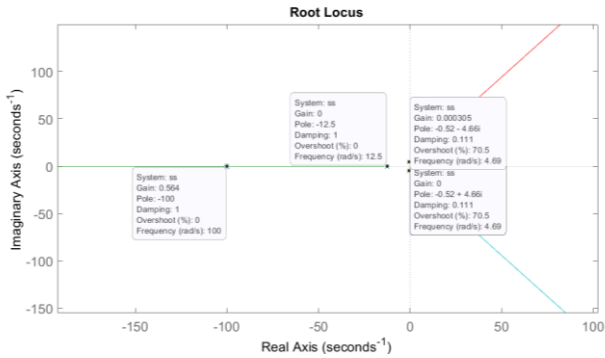**Figure 3.** Block diagram of the AVR system

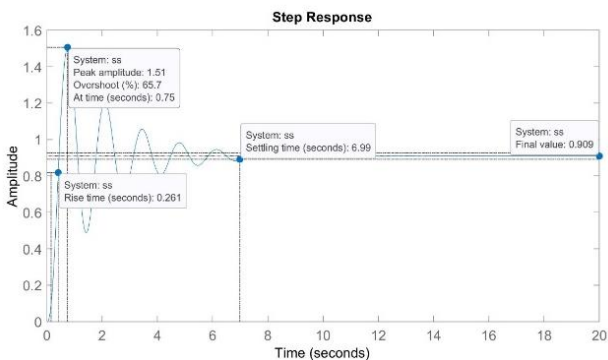**Figure 4.** Root locus of the AVR system without PID controller

Figure 5. Step response of the AVR system

As can be seen from the root locus in Fig. 4, the open loop poles of the AVR system are s_1=-99.97, s_2=-12.4892, $s_{3,4}$=-0.5198±4.6642i, respectively, and their respective damping ratios are 1.000, 1.000, 0.111 and 0.111 respectively. As shown in Fig. 5, the steady-state value, overshoot, rise time, and settling time are 0.909, 65.7%, 0.261 s, and 6.99 s (2% bant), respectively. The steady-state error of the system is obtained as 0.091 pu. So, the system needs to have a controller to eliminate the steady state error and improve the transient response of the system.
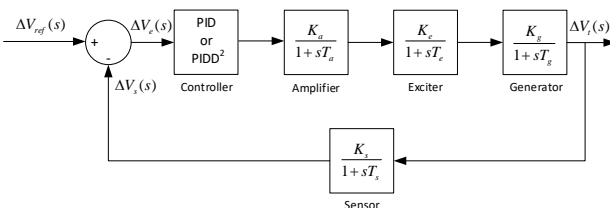

Figure 6. Block diagram of the AVR system with PID or PIDD² controller

The PID and PIDD² controllers are designed to improve the response of the AVR system. The AVR system block diagram with PID and PIDD² controllers is depicted in Fig. 6.

The transfer function for the AVR system with PID and PIDD² controllers depicted in Fig. 6 is defined in Eq. 6 and 7, respectively.

$$\frac{\Delta V_t(s)}{\Delta V_{ref}(s)} = \frac{0.1K_d s^2 + (0.1K_p + 10K_d)s^2 + (0.1K_i + 10K_p)s + 10K_i}{0.0004s^5 + 0.045s^4 + 0.555s^3 + (1.51 + 10K_d)s^2 + (1 + 10K_p)s + 10K_i} \quad (6)$$

$$\frac{\Delta V_t(s)}{\Delta V_{ref}(s)} = \frac{0.1K_{dd}s^4 + (0.1K_d + 10K_{dd})s^3 + (10K_d + 0.1K_p)s^2 + (0.1K_i + 10K_p)s + 10K_i}{0.0004s^5 + 0.0454s^4 + (10K_{dd} + 0.555)s^3 + (10K_d + 1.51)s^2 + (10K_p + 1)s + 10K_i} \quad (7)$$

2.3. Determination of PID and PIDD² parameters, and objective functions

Three optimal control parameters are necessary for the design of the PID controller. The objective function is minimized to estimate these optimum parameters. Several objective functions are considered such as integral of time multiplied absolute error (ITAE), integral of time multiplied square error (ITSE), integral square error (ISE), integral absolute error (IAE), integral of square time multiplied by square error (ISTSE), integral square time multiplied square error (ISTES). The aforementioned objective functions are given in the following equations.

- ITAE

$$J = \int_0^T t|e(t)|dt \quad (8)$$

- ITSE

$$J = \int_0^T t|e^2(t)|dt \quad (9)$$

- ISE

$$J = \int_0^T |e^2(t)|dt \quad (10)$$

- IAE

$$J = \int_0^T |e(t)|dt \quad (11)$$

- ISTSE

$$J = \int_0^T t^2 e^2(t)dt \quad (12)$$

- ISTES

$$J = \int_0^T [t^2 e(t)]^2 dt \quad (13)$$

Where $e = V_r - V_t$, V_t and V_r are the terminal and reference voltage, respectively.
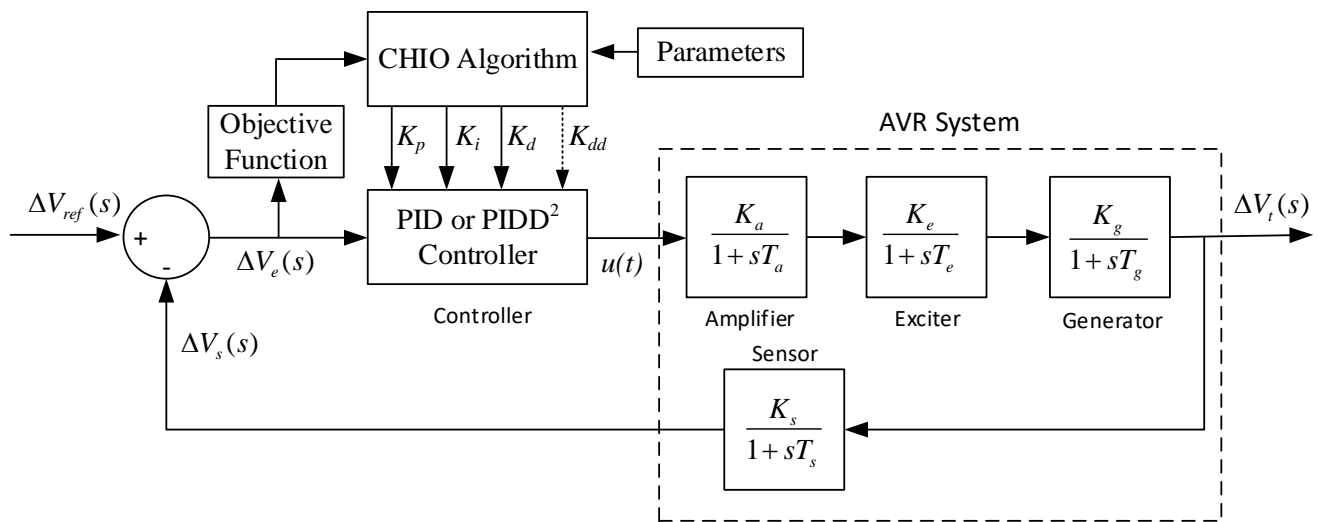
Figure 7. PID or PIDD[2] controlled AVR system with CHIO algorithm

To find out the optimal parameters of the PID or PIDD[2] controllers, the formulation of the optimization problem can be given below.

min J

$$st.x = f(t,u) \tag{14}$$

$$K_{min} < K < K_{max}$$

where J and x are the objective function of optimization problem and system model, respectively. K_{min}-K_{max} are the limits of the controller parameters used as an inequality constraint in optimization problem. K are the controller parameters K_p, K_i, K_d, and K_{dd} in short form.

The CHIO algorithm is used to solve the optimization problem given above and find the optimal controller parameters. Fig. 7 shows the block diagram of the AVR system with the proposed CHIO algorithm tuned PID or PIDD[2] controller.

3. FINDINGS

In the paper, CHIO technique is utilized to obtain the optimal PID controller parameters K_p, K_i, K_d and PIDD[2] controller parameters K_p, K_i, K_d, K_{dd} as shown in Fig. 7. To make a comparison in terms of transient response, different objective functions are used. The optimal parameters of the controllers determined by minimizing several objective functions are given in Table 2.

The implementation of the CHIO algorithm, its adaptation to the AVR system and all analysis have been carried out using MATLAB [25]. Steady-state error, overshoot, settling time, rise time and peak time showing the response and behavior of the AVR system with PID controller designed according to the different objective functions are given in Table 2.
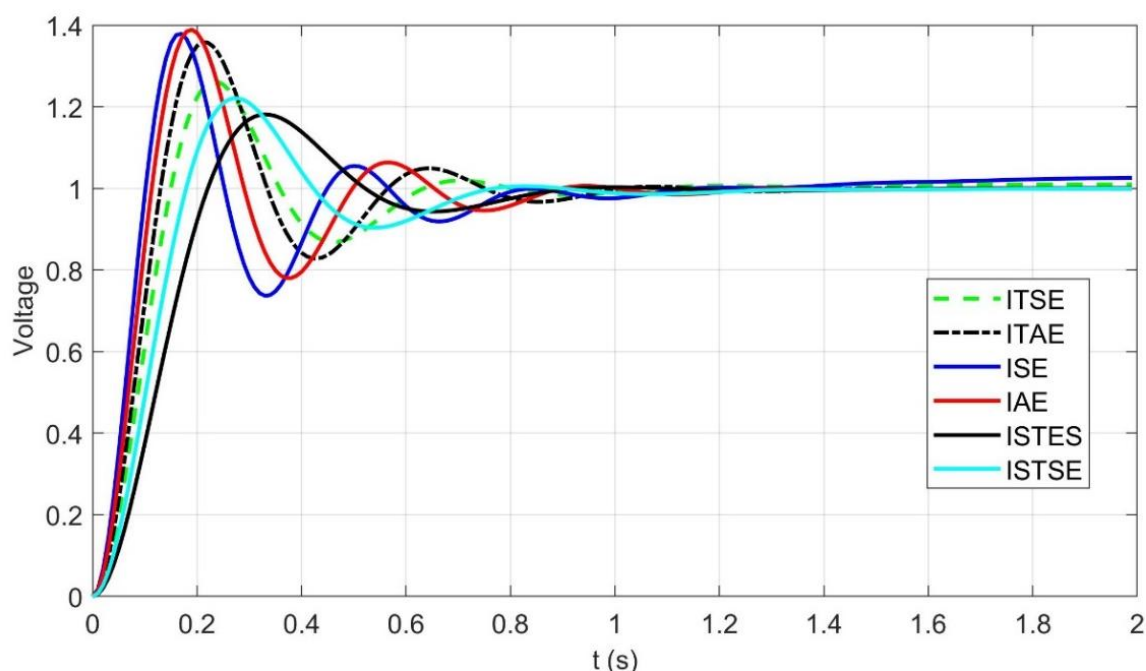

Figure 8. Terminal voltage of the AVR system with CHIO-PID controller for different objective functions.

Table 2. The optimal parameters of CHIO-based PID controllers according to the different objectives

Objective Function / Parameters	K_p	K_i	K_d	Objective Value	M_p (pu)	E_{ss} (pu) (1.8 s)	t_s (s) (2% bant)	t_r (s)	t_p (s)
ITSE	1.5627	1.4835	0.7864	0.00558	1.2617	0.0093	**0.6055**	0.1012	0.23
ITAE	2.3384	1.5386	0.9246	0.0386	1.358	0.0012	0.9307	0.0875	0.21
ISE	1.1141	2.3534	1.4503	0.0652	1.3787	0.022	3.0251	**0.0683**	**0.17**
IAE	2.2532	1.6406	1.1687	0.1619	1.3888	**0.0004**	0.8464	0.0761	0.19
ISTES	1.3269	0.8857	0.4418	0.00024	**1.1811**	0.0013	0.8184	0.1494	0.33
ISTSE	1.5106	1.0075	0.5982	0.00122	1.2208	0.0013	0.7090	0.1210	0.27

Table 3. The optimal parameters of PID controller and transient response results obtained by ITSE with the different approaches.

Controllers / Parameters	K_p	K_i	K_d	M_p (pu)	E_{ss} (pu)	t_s (s) (2% bant)	t_r (s)	t_p (s)	ITSE (t_{sim}=20 s)
CHIO-PID (Proposed)	1.5627	1.4835	0.7864	1.2617	0.0093	**0.6065**	**0.101**	0.23	**0.00558**
KA-PID [7]	1.0685	1.0018	0.5103	**1.136**	0.0129	0.771	0.143	0.31	0.0061
ZN-PID [10]	1.021	1.8743	0.139	1.515	0.00553	3.052	0.237	0.644	0.107
ABC-PID [24]	1.6524	0.4083	0.3654	1.25	0.02684	3.094	0.156	0.36	0.018
LUS-PID [11]	1.2012	0.9096	0.4593	1.156	0.00358	0.800	0.149	0.322	0.0064
PS-PID [3]	1.2771	0.8471	0.4775	1.169	**0.00174**	0.804	0.144	0.316	0.0064
BBO-PID [12]	1.2464	0.5893	0.4596	1.16	0.01564	1.446	0.149	0.317	0.0077

Table 4. The results for CHIO-based PIDD^2 controller with ITAE objective function under different parameter limits.

Constraint / Parameters	K_p	K_i	K_d	K_{dd}	Objective Value	M_p (pu)	E_{ss} (pu) (1.8 s)	t_s (s) (2% bant)	t_r (s)	t_p (s)
0.001 < K < 3	2.9945	1.9947	1.0797	0.079754	0.0015744	1	0	0.1468	0.0839	1.05
0.001 < K < 5	4.9796	3.2962	1.8223	0.1492	0.0008023	1.0002	0	0.0561	0.036	0.73
0.001 < K < 10	9.9334	6.6262	3.5827	0.26644	0.00026937	1.144	0	0.0620	0.0154	0.035

Table 5. The results for CHIO-based PIDD^2 controller with ITSE objective function under different parameter limits.

Constraint / Parameters	K_p	K_i	K_d	K_{dd}	Objective Value	M_p (pu)	E_{ss} (pu) (1.8 s)	t_s (s) (2% bant)	t_r (s)	t_p (s)
0.001 < K < 3	3	2.1396	1.3947	0.12497	0.00027538	1.0021	0.002	0.3777	0.0529	2
0.001 < K < 5	5	3.2073	2.7619	0.26957	0.00011654	1.0983	0.0003	0.2851	0.0159	0.033
0.001 < K < 10	8.804	5.6957	3.0964	0.28613	3.5221e-05	1.1298	0.000177	0.0997	0.0146	0.032

Table 6. The results for CHIO-based PIDD^2 controller with ISE objective function under different parameter limits.

Constraint / Parameters	K_p	K_i	K_d	K_{dd}	Objective Value	M_p (pu)	E_{ss} (pu) (1.8 s)	t_s (s) (2% bant)	t_r (s)	t_p (s)
0.001 < K < 3	3	3	3	0.42594	0.0054334	1.2431	1.7702e-04	0.8645	0.0092	0.022
0.001 < K < 5	5	5	3.3196	0.4366	0.004787	1.2627	0.0053	0.3832	0.0089	0.022
0.001 < K < 10	10	5.301	2.93705	0.444665	0.0044699	1.2604	0.0015	0.1939	0.0087	0.022

Table 7. The results for CHIO-based PIDD^2 controller with IAE objective function under different parameter limits.

Constraint / Parameters	K_p	K_i	K_d	K_{dd}	Objective Value	M_p (pu)	E_{ss} (pu) (1.8 s)	t_s (s) (2% bant)	t_r (s)	t_p (s)
0.001 < K < 3	3	2.0037	1.0903	0.079727	0.0401	1.0001	0	0.1431	0.083	1.91
0.001 < K < 5	5	3.31	1.8359	0.14542	0.0202	1	0	0.0562	0.0367	2
0.001 < K < 10	10	6.659	3.60947	0.27295	0.0128	1.1485	0	0.0604	0015	0.034

Table 8. The results for CHIO-based PIDD^2 controller with ISTES objective function under different parameter limits.

Parameters / Constraint	K_p	K_i	K_d	K_{dd}	Objective Value	M_p (pu)	E_{ss} (pu) (1.8 s)	t_s (s) (2% bant)	t_r (s)	t_p (s)
0.001 < K < 3	2.1485	1.3948	0.8376	0.078934	4.83e-06	1.0042	2.95e-05	0.3939	0.132	2
0.001 < K < 5	5	3.3473	1.7741	0.12287	1.47e-08	1.0178	7.73e-06	0.0629	0.0432	0.101
0.001 < K < 10	7.2514	4.7424	2.7353	0.24268	4.77e-08	1.0821	1.27e-05	0.1091	0.0181	0.037

Table 9. The results for CHIO-based PIDD^2 controller with ISTSE objective function under different parameter limits.

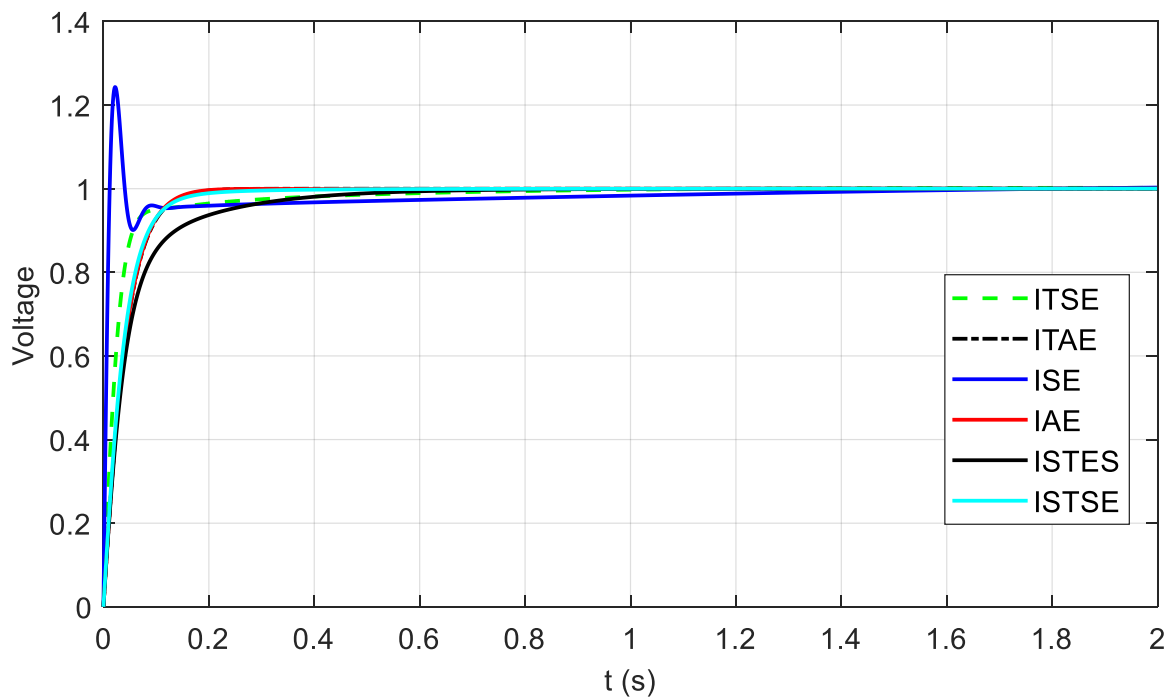| Parameters / Constraint	K_p	K_i	K_d	K_{dd}	Objective Value	M_p (pu)	E_{ss} (pu) (1.8 s)	t_s (s) (2% bant)	t_r (s)	t_p (s)
0.001 < K < 3	3	1.995	1.1051	0.084801	1.4682e-05	1.0001	6.67e-05	0.1583	0.0813	1.93
0.001 < K < 5	5	3.3085	1.8376	0.14435	1.8623e-06	1	5.12e-06	0.0563	0.037	2.87
0.001 < K < 10	7.6209	5.0543	2.7458	0.20872	6.9491e-07	1.007	2.61e-05	0.0706	0.0214	0.045

Figure 9. Terminal Voltage of AVR system with CHIO - PIDD^2 controller (0.001<K<3)
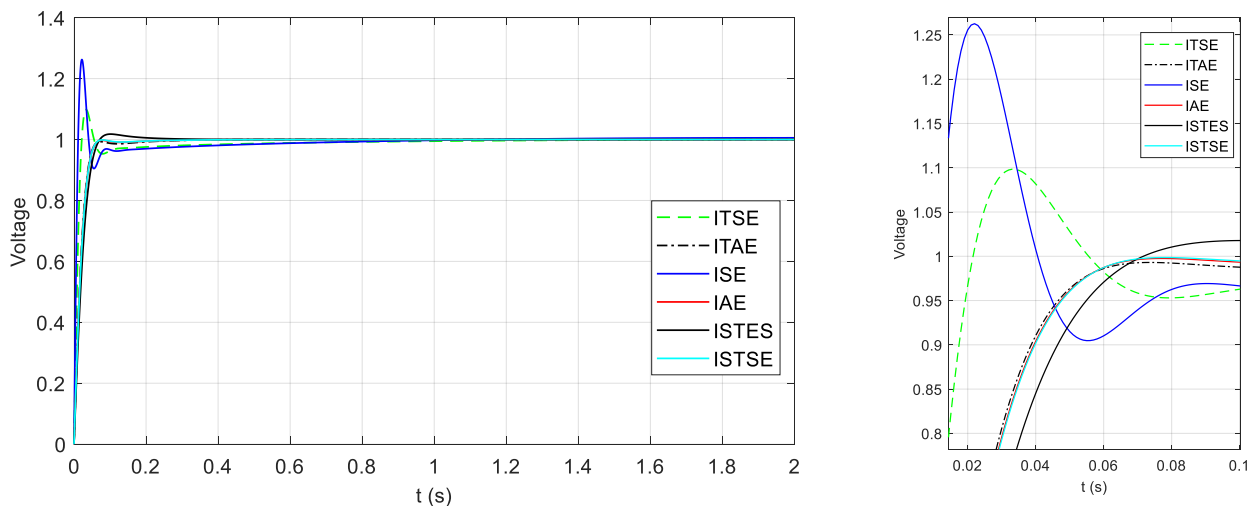

Figure 10. Terminal Voltage of AVR system with CHIO - PIDD^2 controller (0.001<K<5)
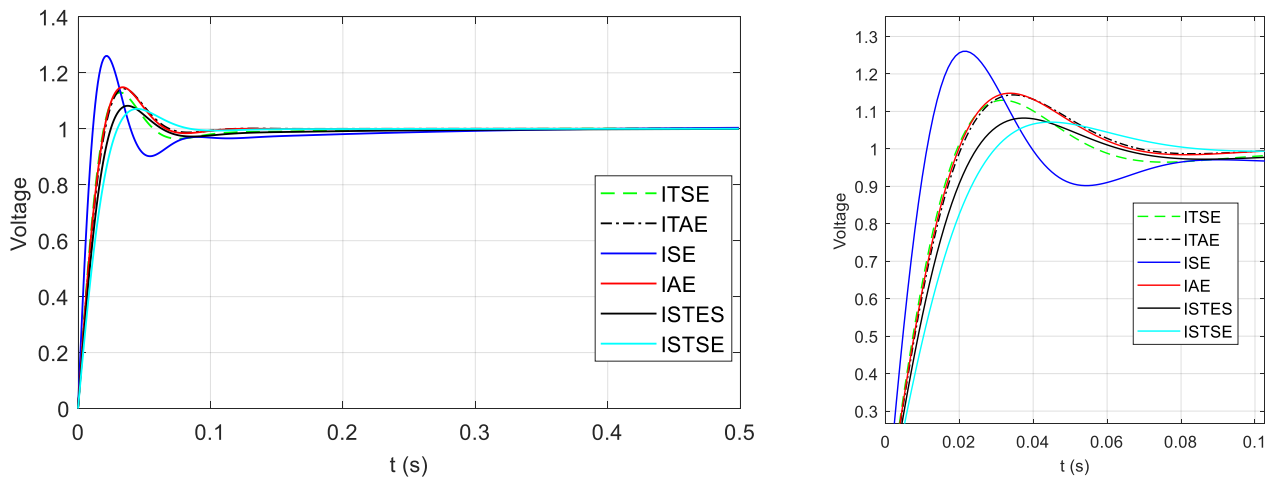
Figure 11. Terminal Voltage of AVR system with CHIO - PIDD^2 controller (0.001<K<10)
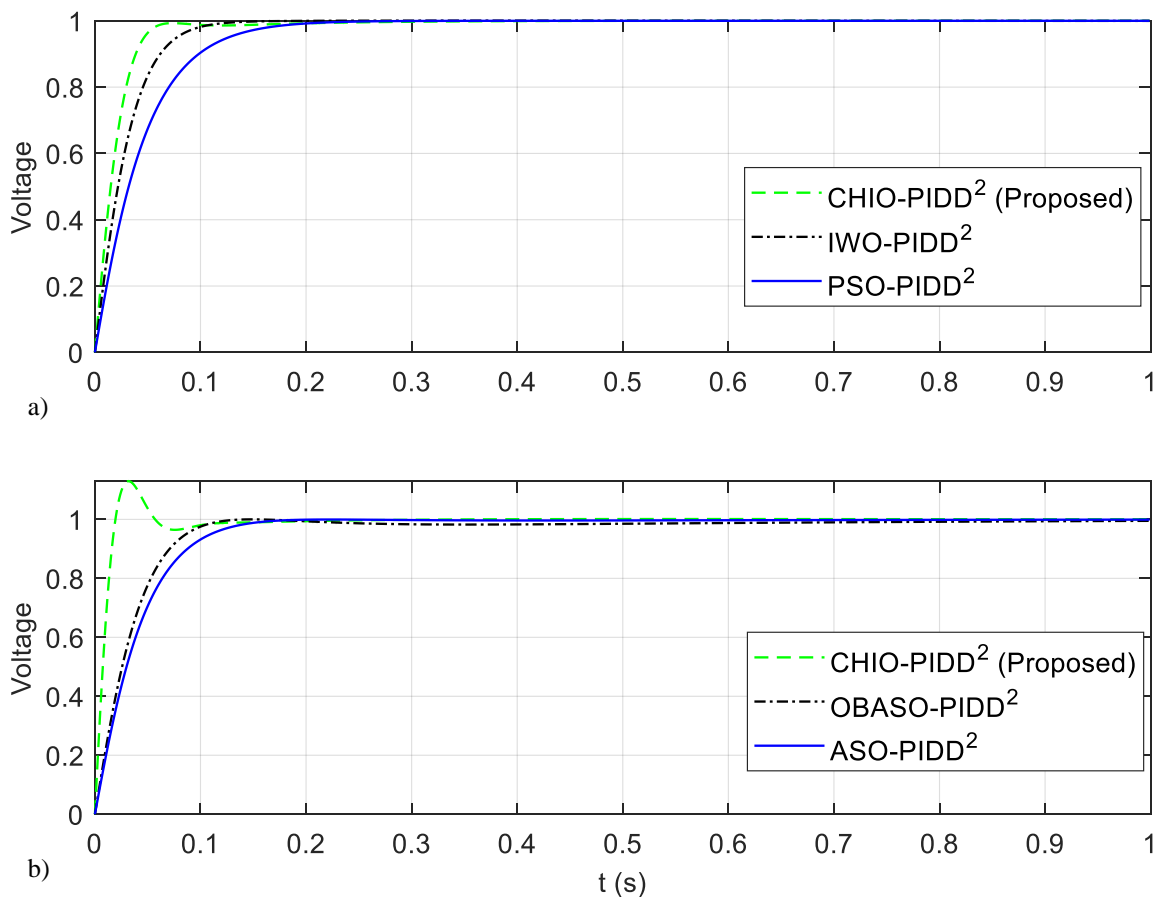

Figure 12. Comparative results of AVR system with ITAE (a) and ITSE (b) objective function

In Tables, the time response characteristic parameters M_p, E_{ss}, t_s, t_r and t_p are the percentage overshoot, steady state error, settling time, rise time and peak time, respectively. The settling time (t_s) is defined as the time within a band of ±2% around the final value of the step response.

To demonstrate the effect of the objective function on the design of controller and controller performance, some objective functions are utilized in the optimization problem.

The optimal parameters obtained with different objective functions are given in Table 2. Objective value, steady state error, maximum overshoot, rise time, settling time, and the peak time for parameters found with each objective function are also given in Table 2. The system responses with these parameters are shown in Fig. 8. Fig. 8 shows the comparative simulation results for the response of the AVR system designed with different objective functions.

Selçuk Emiroğlu, Talha Enes Gümüş

Optimal Control of Automatic Voltage Regulator System with Coronavirus Herd Immunity Optimizer Algorithm-Based PID plus Second Order Derivati...

Table 10. The comparative results for PIDD^2 controller based on different approaches

Parameters / Controllers	K_p	K_i	K_d	K_{dd}	Objective Value	M_p (pu)	E_{ss} (pu) (1.8 s)	t_s (s) (2% bant)	t_r (s)	t_p (s)
CHIO-PIDD^2 (Proposed) - ITAE	4.9796	3.2962	1.8223	0.1492	**0.0008**	1.0002	**0**	**0.0561**	**0.036**	0.73
IWO - PIDD^2 [6]	3.9348	2.5753	1.3985	0.10453	0.0019	1.0007	2.47e-04	0.0981	0.0584	**0.3392**
PSO - PIDD^2 - ITAE [5]	2.7784	1.8521	0.9997	0.07394	0.0018	1	4.29e-06	0.1635	0.0930	0.4295
CHIO - PIDD^2 (Proposed) - ITSE	8.804	5.6957	3.0964	0.28613	**3.52e-05**	1.1298	1.77e-04	**0.0997**	**0.0146**	**0.032**
OBASO - PIDD^2 - ITSE [8]	2.9209	1.9463	1.3359	0.08813	3.56e-04	1.0009	2.75e-04	0.1036	0.0662	2.48
ASO - PIDD^2 - ITSE [8]	2.9310	1.9571	1.1033	0.07771	4.16e-04	**1.0002**	**1.74e-04**	0.1363	0.0825	2.11

In terms of settling time, ITSE objective function gives the shortest settling time as 0.6055 s in 2% bant. In terms of rise time, ISE objective function gives the shortest rise time as 0.0683 s among all objective functions. Also, ISTES and IAE objective functions give the smallest maximum overshoot as 1.1811 pu and steady-state error as 0.0004 pu (at 1.8 s), respectively.

Comparisons are made with other approaches in the literature using ITSE objective function to demonstrate the effectiveness and advantage of the proposed CHIO-PID controller. For comparison, the values which show the system behavior with proposed and other approaches are given in Table 3. As can be seen in Table 3, the proposed CHIO based PID controller gives better results among them. It seems that rise time, settling time, and the peak time is the smallest among the approaches given in Table 3. Especially, ITSE objective value of 0.00558 is the smallest, so the proposed approach provides the minimum objective value.

Tables 4-9 show the results for CHIO-based PIDD^2 controller with different objective functions ITAE, ITSE, IAE, ISE, ISTES and ISTSE under different parameter limits, respectively. It seems that the three different parameter limits are employed for the optimization as an inequality constraint. One can deduce from Tables 4 - 9 that the objective values decrease when the maximum parameters' values are increased for all objective functions. Also, steady state error, settling time, rise time, maximum overshoot, and the peak time of the AVR system with PIDD^2 controller with optimal parameters obtained by using the CHIO algorithm are given in Tables 4 - 9.

Figs. 9- 11 show the transient response of the AVR system with CHIO-based PIDD^2 controller using different objective functions and different parameter limits. Three different parameter limits are used to find the optimal parameters in optimization as a constraint like 0.001<K<3, 0.001<K<5, 0.001<K<10 for the parameters K_p, K_i, K_d, K_{dd}. Fig. 10 shows the comparative results for different PIDD^2 controllers of the AVR system with ITAE and ITSE functions using the parameters given in Table 10. It seems that the system with the proposed approach has a smaller objective value, rise and settling time than the other methods seen in Table 10 and Fig. 12. In addition, the system with the proposed approach used in ITSE objective function has a little bit larger maximum overshoot. However, the objective function value, settling time, and rise time are the smallest among them.
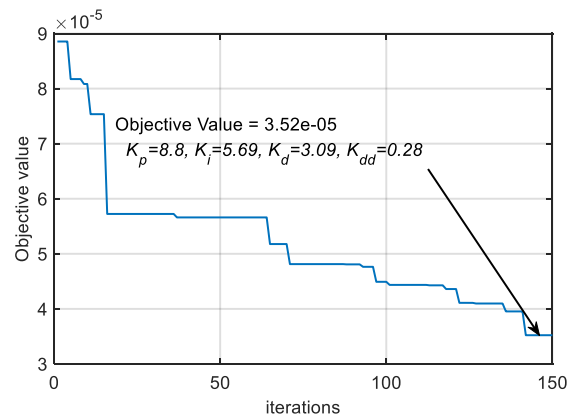
Figure 13. Convergence characteristic for CHIO-PIDD^2 (Proposed approach) using ITSE.

It is compared with other approaches given in Table 10 to demonstrate the effectiveness and advantage of the proposed CHIO-PIDD^2 controller, which improves the AVR system's transient response.

Also, objective value versus iteration graph is given in Fig. 13. The convergence behavior of CHIO algorithm for PIDD^2 controller based on ITSE as in Table 10 can be seen in Fig. 13.

In simulations, the parameters of CHIO are taken as 100 for the population size, 100 for the Max age, with a spreading rate equal to 0.1.

4. DISCUSSION AND CONCLUSION

In this paper, a recently proposed CHIO algorithm is used to obtain the optimal parameters of PID and PID plus second-order derivative (PIDD^2) controllers. Different objectives are investigated to demonstrate the effect of objective functions on the design of PID and PIDD^2 controllers. Furthermore, the proposed CHIO-based PID and PIDD^2 controllers and other optimization algorithm-based PID and PIDD^2 controllers such as ASO, OBASO, PSO, IWO, ABC, KA, DE, ZN, LUS, BBO and PS etc. have been compared and shown in figures and tables.

The response of the AVR system is improved with the proposed approach in terms of rise time, settling time, and maximum overshoot compared to approaches cited in the paper. Simulation results showed that proposed PID and PIDD^2 controllers provide superior response performance.

Selçuk Emiroğlu, Talha Enes Gümüş

Optimal Control of Automatic Voltage Regulator System with Coronavirus Herd Immunity Optimizer Algorithm-Based PID plus Second Order Derivati...

Author contributions: Concept – S.E, T.E.G; Data Collection &/or Processing – S.E, T.E.G; Literature Search – S.E, T.E.G; Writing – S.E, T.E.G

Conflict of Interest: No conflict of interest was declared by the authors.

Financial Disclosure: The authors declared that this study has received no financial support.

REFERENCES

[1] P. Kundur, Power System Stability and Control, vol. 20073061. McGraw-Hill, 1994.

[2] H. Saadat, Power System Analysis. PSA Publishing LLC, 2011.

[3] B. K. Sahu, P. K. Mohanty, and N. Mishra, "Robust Analysis and Design of PID controlled AVR system using Pattern Search algorithm," in IEEE International Conference on Power Electronics, Device and Energy System 2012, 2012.

[4] S. Panda, B. K. Sahu, and P. K. Mohanty, "Design and performance analysis of PID controller for an automatic voltage regulator system using simplified particle swarm optimization," J. Franklin Inst., vol. 349, no. 8, pp. 2609–2625, 2012.

[5] M. A. Sahib, "A novel optimal PID plus second order derivative controller for AVR system," Eng. Sci. Technol. an Int. J., vol. 18, no. 2, pp. 194–206, 2015.

[6] D. Mokeddem and S. Mirjalili, "Improved Whale Optimization Algorithm applied to design PID plus second-order derivative controller for automatic voltage regulator system," J. Chinese Inst. Eng. Trans. Chinese Inst. Eng. A, vol. 43, no. 6, pp. 541–552, 2020.

[7] S. Ekinci, A. Demirören, H. L. Zeynelgil, and S. Kaya, "Böbrek-ilhamlı Algoritma ile Otomatik Gerilim Regülatör Sistemi için PID Kontrolör Tasarımı," Gazi Üniversitesi Fen Bilim. Derg. Part C Tasarım ve Teknol., vol. 7, no. 2, pp. 383–398, 2019.

[8] S. Ekinci, A. Demirören, H. L. Zeynelgil, and B. Hekimoğlu, "An opposition-based atom search optimization algorithm for automatic voltage regulator system," J. Fac. Eng. Archit. Gazi Univ., vol. 35, no. 3, pp. 1141–1157, 2020.

[9] M. Micev, M. Ćalasan, Z. M. Ali, H. M. Hasanien, and S. H. E. Abdel Aleem, "Optimal design of automatic voltage regulation controller using hybrid simulated annealing – Manta ray foraging optimization algorithm," Ain Shams Eng. J., vol. 12, no. 1, pp. 641–657, 2021.

[10] B. Hekimoğlu and S. Ekinci, "Grasshopper optimization algorithm for automatic voltage regulator system," 2018 5th Int. Conf. Electr. Electron. Eng. ICEEE 2018, pp. 152–156, 2018.

[11] P. K. Mohanty, B. K. Sahu, and S. Panda, "Tuning and assessment of proportional-integral-derivative controller for an automatic voltage regulator system employing local unimodal sampling algorithm," Electr. Power Components Syst., vol. 42, no. 9, pp. 959–969, 2014.

[12] U. Güvenç, T. Yiğit, A. H. Işık, and I. Akkaya, "Performance analysis of biogeography-based optimization for automatic voltage regulator system," Turkish J. Electr. Eng. Comput. Sci., vol. 24, no. 3, pp.

1150–1162, 2016.

[13] M. S. Ayas and E. Sahin, "FOPID controller with fractional filter for an automatic voltage regulator," Comput. Electr. Eng., vol. 90, no. April 2020, p. 106895, 2021.

[14] A. Sikander, P. Thakur, R. C. Bansal, and S. Rajasekar, "A novel technique to design cuckoo search based FOPID controller for AVR in power systems," Comput. Electr. Eng., vol. 70, pp. 261–274, 2018.

[15] A. J. H. Al Gizi, "A particle swarm optimization, fuzzy PID controller with generator automatic voltage regulator," Soft Comput., vol. 23, no. 18, pp. 8839–8853, 2019.

[16] M. H. Suid and M. A. Ahmad, "Optimal tuning of sigmoid PID controller using Nonlinear Sine Cosine Algorithm for the Automatic Voltage Regulator system," ISA Trans., vol. 128, pp. 265–286, 2022.

[17] M. A. Labbaf Khaniki, M. Behzad Hadi, and M. Manthouri, "Feedback Error Learning Controller based on RMSprop and Salp Swarm Algorithm for Automatic Voltage Regulator System," 2020 10h Int. Conf. Comput. Knowl. Eng. ICCKE 2020, pp. 425–430, 2020.

[18] V. Sharma, V. Kumar, R. Naresh, and V. Kumar, "Automatic voltage regulator system with state-feedback and PID based sliding mode control design," Proc. 2021 1st Int. Conf. Adv. Electr. Comput. Commun. Sustain. Technol. ICAECT 2021, 2021.

[19] M. A. Al-Betar, Z. A. A. Alyasseri, M. A. Awadallah, and I. Abu Doush, "Coronavirus herd immunity optimizer (CHIO)," Neural Comput. Appl., vol. 33, no. 10, pp. 5011–5042, 2021.

[20] L. M. Dalbah, M. A. Al-Betar, M. A. Awadallah, and R. A. Zitar, "A modified coronavirus herd immunity optimizer for capacitated vehicle routing problem," J. King Saud Univ. - Comput. Inf. Sci., vol. 34, no. 8, pp. 4782–4795, 2022.

[21] M. Alweshah, S. Alkhalaileh, and M. A. Al-betar, "Coronavirus herd immunity optimizer with greedy crossover for feature selection in medical diagnosis," Knowledge-Based Syst., vol. 235, p. 107629, 2022.

[22] M. Alqarni, "Sodium sulfur batteries allocation in high renewable penetration microgrids using coronavirus herd immunity optimization," Ain Shams Eng. J., vol. 13, no. 2, p. 101590, 2022.

[23] S. Amini, S. Ghasemi, H. Golpira, and A. Anvari-moghaddam, "Coronavirus Herd Immunity Optimizer (CHIO) for Transmission Expansion Planning," in 2021 IEEE International Conference on Environment and Electrical Engineering and 2021 IEEE Industrial and Commercial Power Systems Europe (EEEIC / I&CPS Europe), 2021, no. 18.

[24] H. Gozde and M. C. Taplamacioglu, "Comparative performance analysis of artificial bee colony algorithm for automatic voltage regulator (AVR) system," J. Franklin Inst., vol. 348, no. 8, pp. 1927–1946, 2011.

[25] "MATLAB." The Mathworks, Inc., Natick, Massachusetts, United States.